Mathematical Models and Methods in Applied Sciences

Waves for an hyperbolic Keller-Segel model and branching instabilities

Fiammetta Cerreti

(1) UPMC, CNRS UMR 7598, Laboratoire Jacques-Louis Lions, F-75005, Paris.
Email: fiam.cer@gmail.com

Benoît Perthame[(1)(2)]

(2) INRIA Paris-Rocquencourt, Equipe BANG.
Email: benoit.perthame@upmc.fr

Christian Schmeiser

Faculty for Mathematics, University of Vienna, Austria, and RICAM, Linz, Austria.
Email: christian.schmeiser@univie.ac.at

Min Tang[(2)]

Email: tangmin1002@gmail.com

Nicolas Vauchelet[(1)(2)]

Email: nicolas.vauchelet@upmc.fr

Received (Day Month Year)
Revised (Day Month Year)
Communicated by (xxxxxxxxxx)

Recent experiments for swarming of the bacteria *Bacillus subtilis* on nutrient rich media show that these cells are able to proliferate and spread out in colonies exhibiting complex patterns as dendritic ramifications. Is it possible to explain this process with a model that does not use local nutrient depletion?

We present a new class of models which is compatible with the experimental observations and which predict branching instabilities and does not use nutrient limitation. These conclusions are based on numerical simulations. The most complex of these models is also the biologically most accurate but the essential effects can also be obtained in simplified versions which are amenable to analysis. An example of instability mechanism is the transition from a shock wave to a rarefaction wave in a reduced two by two hyperbolic system.

Keywords: Keller-Segel system, hyperbolic system, shock waves, branching instability, cell communities.

AMS Subject Classification:
35L45, 35L67, 65M99, 92C17

1. Introduction

The motivation of this work comes from recent experiments and measurements on swarming of the bacteria *Bacillus subtilis* reported in [10,15,16]. It is observed that, when inoculated on nutrient rich media, these cells are able to proliferate and spread out in colonies exhibiting complex patterns as dendritic ramifications. This occurs under the effect of cellular communication through excretion of signalling molecules. Collective behaviours like this are, however, poorly understood and this has initiated the research field of 'cell communities self-organization' (sometimes also called socio-microbiology), a vast subject which can also be related to fluid flows [27].

In the first phase of a typical experiment, an inoculum of cells proliferates and grows into a so called *mother colony*. After a sudden bursting phenomenon, a number of (primary) dendrites grows from the mother colony. Dendrites typically contain two different types of cells: highly motile *swarmers* in the tip and *supporters* with significantly smaller motility in the stem. The supporters are maintained at a constant density. Subsequent branching events create complicated patterns. Other observations are the creation of *surfactin* at least by the mother colony, which is essential for the process, the preference of the dendrites for the radial direction, and the tendency of dendrites to avoid each other. Finally, the experiments have been carried out on nutrient rich substrates and seem to indicate that the whole process is not nutrition limited.

This final observation leads to the essential contribution of this work. As observed in [21], all past attempts to model branching patterns for *B. subtilis* are based on the assumption of a nutrition limited process (see [19,23,17,8] and the survey in [24]). Most of them are related to dynamical pattern formations *à la* Gray-Scott [9]. Continuing the arguments in [21], a new class of models will be presented, which is compatible with the experimental results, which predicts branching, and which assumes abundance of nutrient. The most complex of these models (which we call the 'full model') is also the biologically most accurate. It will be shown, however, that the essential effects can also be observed in simplified versions which are amenable to analysis.

The most important part of the full model is the description of the swarmer dynamics. On the one hand it is assumed that surfactin acts on them like a chemorepellent, on the other hand cell-cell signaling by a chemoattractant is assumed, which has the effect to keep the group of swarmers together as observed in experiments. To prevent overcrowding, a density dependent chemotactic sensitivity is used turning off the chemotactic effect when a critical density is reached.

Neglecting the effect of surfactin, the model for swarmers is reminiscent of the usual Keller-Segel model with source (see [13,14,12,23,25,?] and the references therein) for cell aggregation, however without diffusion effects and with prevention of overcrowding. Indeed, in the absence of surfactin, this system has been studied, both theoretically and numerically by several authors [3,4,6,7]. In any dimension, solu-

tions exist that stay bounded. They exhibit a coarsening process reminescent of phase change models, where plateau-like peaks of the cell density form after a short transient period leading to sharp fronts (shock waves). With a small diffusion of the cells, these 'plateaus' (along with the terminology of [11]) merge with an exponentially slow dynamics. In the present paper, the question is to understand the dynamics of the plateaus resulting from the repellent forces.

Swarmer cells are assumed to multiply, but we assume that after division, one of the two daughter cells becomes a supporter. This assumption is based on the experimental observation that the number of swarmers seems to remain constant during dendrite elongation. Two possible mechanisms for maintaining the observed constant supporter density are considered: either diffusion with a diffusivity proportional to the density of a trace substance produced by the swarmers (which we consider the biologically more sound alternative), or a logistic birth-death process. The mother colony is formed of cells packed in a multilayer. They are supposed immotile and do not multiply. Thus, they are represented as a group of 'frozen' cells.

For the dynamics of surfactin, production by the mother colony and by the supporters is assumed, as well as decay and diffusion. Production by the mother colony followed by diffusion should induce the preferred radial direction of the dendrites. Production by the supporters is motivated by the experimental observation that long enough dendrites, which are separated from the mother colony, keep extending and splitting. The chemoattractant is (obviously) produced by the swarmers, and diffuses fast enough for its density to maintain a quasi-steady state, balancing production, diffusion, and decay.

Several of our modeling assumptions are questionable and certainly not sufficiently supported by experimental evidence. On the other hand, we are not aware of any contradictions to experimental observations. Our purpose is to understand, if these ingredients are enough to predict the growth and branching of dendrites. Our analysis has to be understood as purely qualitative. We shall work with a nondimensionalized model, where no effort has been undertaken to identify realistic parameter values.

In Section 2, we formulate the full model and present several numerical simulations, showing that dendrite growth and branching can be predicted. One aspect, namely dendrite growth, can be explained analytically for a strongly simplified model. This is done in Section 3 in the form of a traveling wave analysis. The simplified model is one-dimensional, neglects supporters and the mother colony, and assumes that surfactin is produced by the swarmers. Growth of a dendrite is then represented by a moving plateau solution, which can be given analytically in the limit of vanishing surfactin diffusivity. It turns out that such a solution is only stable for strong enough chemoattraction. This analysis will be continued in a more mathematical paper [26]. Finally, in Section 4, three different simplified models are solved numerically showing that splitting of plateaus, i.e. branching of dendrites, seems to be a rather generic consequence of the competition between cell aggregation and

the dispersive effect of surfactin.

2. The full model: mother colony, supporters, swarmers

According to the assumptions formulated in the previous section, the full model has the form

$$\left.\begin{aligned} &\partial_t n + \nabla \cdot \big[n(1-n)\nabla c - n\nabla S\big] = 0,\\ &-D_c \Delta c + \tau_c c = \alpha_c n,\\ &\partial_t S - D_s \Delta S + \tau_s S = \alpha_s m_{col} + \alpha_f f,\\ &\partial_t D_m = d_m n,\\ &\partial_t f - \nabla \cdot (D_m \nabla f) = B_f f(1-f) + B_n n, \end{aligned}\right\} \tag{2.1}$$

where all quantities are dimensionless. We have denoted the unknowns by

- $n(x,t)$ the density of swarmers, for which we consider a conservation equation (explained by the assumption that cell division always produces one swarmer and one supporter cell). The swarmers move under the effect of surfactin (with density S) acting as a chemorepellent, and of a chemoattractant (with density c), which has the effects of holding together the swarmer cells forming the tips of dendrites and of cooperating with S in the splitting mechanism.
- $c(x,t)$ the chemical concentration of the chemoattractant, which is produced by the swarmers with a rate α_c. It diffuses with diffusivity D_c and is degraded with rate τ_c. This reaction-diffusion process is assumed to be fast compared to the other effects and therefore modeled to be in a quasi-steady state.
- $S(x,t)$ the surfactin density that is released by both supporters and by the mother colony with rates α_f and, respectively, α_s. It diffuses with diffusivity D_s, and it is degraded with a rate τ_s. The cell density $m_{col}(x)$ of the mother colony is assumed as fixed and given.
- $D_m(x,t)$ the density of a trace substance left by the swarmers. It is released with a rate d_m.
- $f(x,t)$ the density of supporters, which are produced by cell division of swarmers with rate B_n, diffuse with diffusivity D_m, and reproduce with the logistic rate $B_f(1-f)$. The last two effects, both providing a tendency to make the supporter density constant, will be considered alternatively.

Auxiliary conditions and parameter values: For numerical purposes, the system is considered in a bounded domain $\Omega = [0,L]^2 \subset \mathbb{R}^2$ subject to homogeneous Neumann boundary conditions for c, S, and f, implying also zero flux through the boundary (and therefore no necessity for boundary conditions) for the swarmer density n.

We have performed simulations with $\Omega = [0,4]^2$. We chose the parameter values $D_c = 0.001$, $\tau_c = 1$, $\alpha_c = 1$, $D_s = 0.5$, $\tau_s = 10$, $\alpha_s = 2$, $\alpha_f = 30$, $d_m = 50$, $B_f = 0$, $B_n = 1$. The small value of D_c (together with the moderate value of τ_c) has the consequence that the chemoattraction between swarmer cells is a short range effect. The mother colony is located around the lower left corner with a density given by $m_{col}(x) = 3\mathbb{1}_{|x|\leq 0.4}$. The initial data can be seen as a caricature of the situation immediately after bursting with a small swarmer region next to the mother colony: $n(x,0) = \mathbb{1}_{0.4\leq|x|\leq 0.5}$, $D_m(x,0) = f(x,0) = 0$, and $S(x,0) = S_0(x)$, solving the problem

$$-D_s\Delta S_0 + \tau_s S_0 = \alpha_s m_{col}\,,$$

subject to homogeneous Neumann boundary conditions. This assumes that, previous to bursting, the time of production of surfactin by the mother colony was sufficiently long to produce an equilibrium.

Numerical scheme: The numerical simulation of system (2.1) faces a major difficulty, which is the diversity of mathematical structures with hyperbolic and parabolic or elliptic equations. For this reason we have used two different approaches; the finite volume method on a rectangular grid is more acurate for the hyperbolic equations while a finite element method is better fit to diffusion equations. We use compatible grids to combine both.

We first discretize the square domain $[0,L]\times[0,L]$ with structured rectangles by introducing the nodes $(x_i,y_j) = (i\Delta x, j\Delta y)_{(i,j)\in\mathbb{N}^2}$. Each rectangle can be split into two rectangular triangles which will be referred to as the triangular mesh. A decoupled time-stepping approach is applied, where the equations in (2.1) are solved consecutively. Assume that c, S and f are known on the nodes of the mesh. We compute the gradients ∇c and ∇S thanks to the approximation

$$\partial_x c(x_i,y_j) = \frac{c(x_{i+1},y_j) - c(x_{i-1},y_j)}{2\Delta x} + O(\Delta x^2).$$

Then the hyperbolic conservation law for n is discretized by a first order finite volume Engquist-Osher-type scheme [2] on the rectangular grid. For stability, we impose the CFL (Courant-Friedrichs-Levy) condition $\Delta t < \Delta x/(\max|\nabla S| + \max|\nabla c|)$. Then it is possible to compute the trace D_m directly and we use implicit in time Euler scheme.

For the discretization of the parabolic/elliptic equations for c, S and f, we make use of the general Finite Element package FreeFem++ (see [1]) on the triangular grids. Since n and D_m are known on the nodes of the mesh, an implicit Euler discretization in time is used for the equation for S and f; then a P^1 finite element discretization is performed to find an approximation of c, S and f. All this is built in FreeFEM++.

Finally the algorithm is the following. Assume all quantities are known at time t_k. We first compute the cell density n at time t_{k+1}. Then, an implicit in time Euler

scheme gives D_m at time t_{k+1}. We are yet able to solve the equation for c, S and f and go to the next step.

Results: The results are shown in Figure 1, where we depict five snap shots of the simulation. With our choice of parameters, the swarmer cells form a plateau traveling outwards (in accordance with the traveling wave analysis in Section 3). Additionally, one can observe successive branching, which is compatible with the experimental observations. The main branching mechanism seems to be stable and is kept with $B_f \neq 0$. This mechanism, since it does not use local nutrient depletion, is very different from that observed for reaction-diffusion systems (see [19,23,17,8] and the references therein). The system (2.1) can generate several types of instabilities and we study some of them below for simplified equations.

3. Traveling plateaus in one dimension for small surfactin diffusivity

In order to explain the branching instabilities that occur in (2.1) as shown in Figure 1, a simplification of the full model is introduced. The supporters and the mother colony are not represented, and we assume that the surfactin is solely produced by the swarmers. The resulting model has the form

$$\left.\begin{aligned} &\partial_t n + \nabla \cdot \big(n(1-n)\nabla c - n\nabla S\big) = 0\,, \\ &-D_c \Delta c + \tau_c c = n\,, \\ &\partial_t S - D_S \Delta S = \alpha n\,. \end{aligned}\right\} \tag{3.1}$$

Thus, we just analyze the effect of repellent forces when added to the hyperbolic Keller-Segel model proposed in [7], see also similar models with diffusion in [12] and the references therein. This system is interesting in itself and shares similarities with models for crowds derived by various authors [5,22], although key ingredients are different.

We shall study planar traveling waves. More precisely, we are interested in understanding the capability of the system to produce plateau waves, and in the stability and instability mechanisms involved in the multidimensional dynamics of these waves.

The hyperbolic Keller-Segel system generates plateaus as we explained earlier. The main property of system (3.1) is to create traveling plateaus and, in one space dimension when the repellent signal S does not diffuse, we can give an explicit analytical form of these plateaus. More interesting is their stability, whose analysis is facilitated by a change of unknowns, where (3.1) (with $D_S = 0$) is transformed into an hyperbolic system (with nonlocal coupling), as it was done in [20] for the Keller-Segel system with a nutrient. With $x \in \mathbb{R}$ and with the new variable $v = -\partial_x S$, the

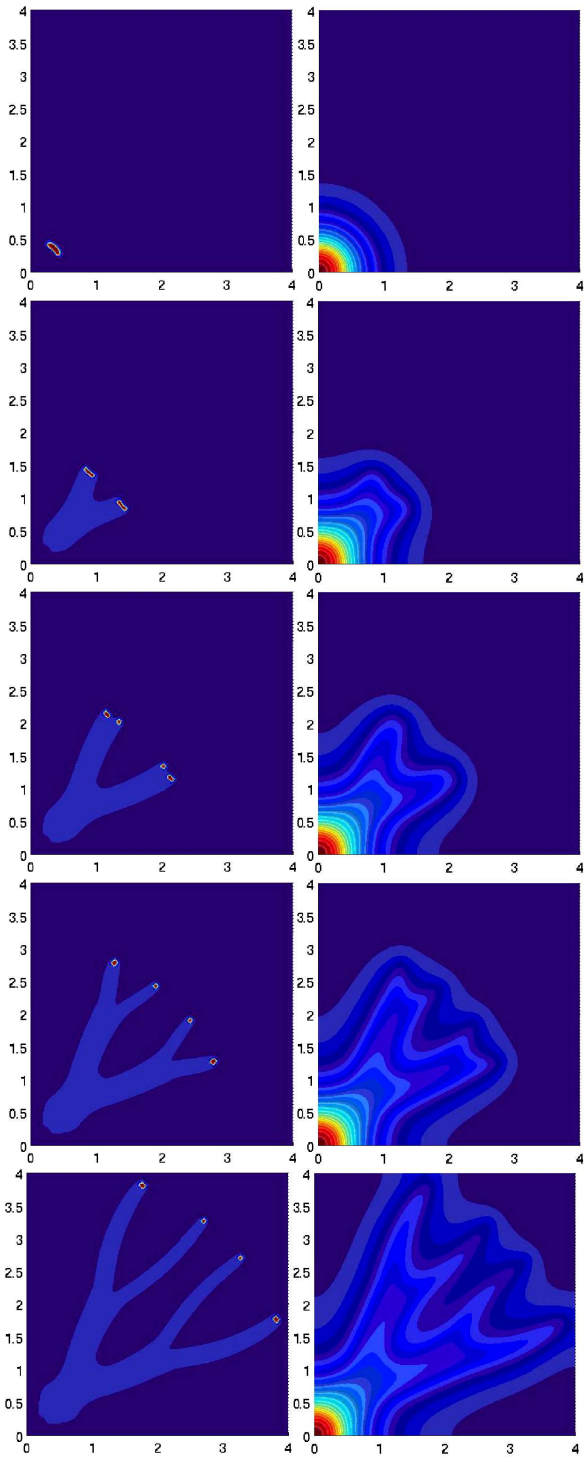

Figure 1. Time dynamic of swarmers and supporters density (left) and of the surfactin concentration S (right) computed with the model (2.1).

system (3.1) becomes

$$\left.\begin{aligned} &\partial_t n + \partial_x\big((n(1-n)\partial_x c + nv\big) = 0\,,\\ &\partial_t v + \partial_x(\alpha n) = D_S\partial_x^2 v\,,\\ &-D_c\partial_x^2 c + \tau_c c = n\,. \end{aligned}\right\} \tag{3.2}$$

Traveling plateaus for vanishing surfactin diffusivity

We set $D_S = 0$ and look for traveling waves with speed σ, which are solutions of the form $n(x-\sigma t)$, $v(x-\sigma t)$, $c(x-\sigma t)$ and, thus, have to satisfy

$$\begin{aligned} &-\sigma n' + \big(n(1-n)c' + nv\big)' = 0\,,\\ &-\sigma v' + \alpha n' = 0\,,\\ &-D_c c'' + \tau_c c = n\,, \end{aligned} \tag{3.3}$$

where the prime denotes differentiation with respect to $y = x - \sigma t$. The first two equations of (3.2) with $D_S = 0$ and with c considered as given are a nonlinear system of hyperbolic conservation laws. For the computation of weak solutions of the traveling wave system (3.3), smooth parts of solutions can be connected by jump discontinuities of n and v, satisfying the Rankine-Hugoniot conditions

$$\sigma[n] = [n(1-n)\partial_y c + nv]\,, \qquad \sigma[v] = [\alpha n]\,, \tag{3.4}$$

where the bracket denotes the jump across a discontinuity. A traveling plateau solution that vanishes outside of a bounded interval, then has to satisfy

$$n\big(-\sigma + (1-n)c' + v\big) = 0\,, \qquad -\sigma v + \alpha n = 0\,. \tag{3.5}$$

Therefore, the nontrivial constant solution $(n, v) = (1, \sigma)$ exists, if its speed satisfies $\sigma^2 = \alpha$, and it can be connected to the state $(n, v) = (0, 0)$. In the following, without loss of generality, positive wave speeds will be considered. The above states are not influenced by the chemoattractant density, which can be computed separately. Thus, we conclude:

Theorem 3.1 (Existence of traveling plateau solutions). *For every $L > 0$, the traveling plateau with speed $\sigma = \sqrt{\alpha}$ and width L,*

$$n(y) = \begin{cases} 1 & \text{for } 0 \le y \le L\,,\\ 0 & \text{otherwise,} \end{cases} \qquad v(y) = \begin{cases} \sqrt{\alpha} & \text{for } 0 \le y \le L\,,\\ 0 & \text{otherwise,} \end{cases}$$

with the chemoattractant concentration given by

$$c(y) = \begin{cases} e^{\mu y}(1 - e^{-\mu L})/(2\tau_c) & \text{for } y < 0\,,\\ (1 - e^{\mu(y-L)}/2 - e^{-\mu y}/2)/\tau_c & \text{for } 0 \le y \le L\,,\\ e^{-\mu y}(e^{\mu L} - 1)/(2\tau_c) & \text{for } y > L\,, \end{cases} \qquad \mu = \sqrt{\tau_c/D_c}\,,$$

is a weak solution of (3.3).

The parameter L can be interpreted as the total number of cells since $L = \int n(y)dy$. This is, together with the usual translational invariance, the only free parameter for the traveling wave. The surfactin concentration can be computed by integration:

$$S(y) = \begin{cases} \sqrt{\alpha}L & \text{for } y < 0\,, \\ \sqrt{\alpha}(L-y) & \text{for } 0 \le y \le L\,, \\ 0 & \text{for } y > L\,. \end{cases}$$

Surfactin is produced inside the plateau, and a trace of surfactin is left behind.

Each plateau wave contains two shock waves. These are only practically relevant, if they are stable, i.e. they have to satisfy an entropy condition. For the purpose of checking this, we need the spectral properties of the Jacobian

$$D_{n,v}f = \begin{pmatrix} (1-2n)c' + v & n \\ \alpha & 0 \end{pmatrix}, \tag{3.6}$$

of the flux vector $f = (n(1-n)c' + nv, \alpha n)$. In these computations, c' can be considered as a given constant, since it is continuous across shocks. The eigenvalues are given by

$$\lambda_\pm(n,v) = \frac{1}{2}\left((1-2n)c' + v \pm \sqrt{\left((1-2n)c'+v\right)^2 + 4\alpha n}\right), \tag{3.7}$$

implying that the flux is strictly hyperbolic as long as $(n,v) \neq (0,-c')$, which holds along the plateau waves, since $c' \neq 0$ for $y < 0$ and for $y > L$. We have $\lambda_+ \ge 0$, $\lambda_- \le 0$. An eigenvector corresponding to eigenvalue λ is given by $r = (\lambda, \alpha)$.

The Hugoniot locus of the origin $(n,v) = (0,0)$ (i.e. the set of all states reachable by a shock) is determined by elimination of the shock speed σ from (3.5). It consists of the v-axis with constant shock speed $\sigma = 0$, implying that the corresponding field is linearly degenerate, and of the curve determined by

$$\alpha n - v(1-n)c' - v^2 = 0\,. \tag{3.8}$$

A tangent vector at the origin is given by (c', α), which has to be collinear to one of the eigenvectors. Since

$$\lambda_+(0,0) = \max\{0, c'\}\,, \qquad \lambda_-(0,0) = \min\{0, c'\}\,,$$

curve (3.8) belongs to the $(+)$-field for $c' > 0$ and to the $(-)$-field for $c' < 0$. Since

$$c'(0) = \frac{1 - \exp\left(-L\sqrt{\tau_c/D_c}\right)}{2\sqrt{\tau_c D_c}} > 0\,,$$

the shock at $y = 0$ belongs to the $(+)$-field, and the Lax entropy condition $\lambda_+(1,\sqrt{\alpha}) < \sigma < \lambda_+(0,0)$ is satisfied iff $\partial_y c > \sqrt{\alpha}$.

For the shock at $y = L$ the Hugoniot locus of the state $(n,v) = (1,\sqrt{\alpha})$ has to be examined using $c'(L) < 0$. This shock also belongs to the $(+)$-field, and the entropy

condition now takes the form $\lambda_+(0,0) = 0 < \sigma < \lambda_+(1,\sqrt{\alpha})$, which is satisfied unconditionally.

We collect our results:

Theorem 3.2 (Stability of traveling plateau solutions). *For dynamic stability of the traveling plateau solutions of Theorem 3.1 (as solutions of* (3.2)*),*

$$c'(0) = \frac{1 - \exp\left(-L\sqrt{\tau_c/D_c}\right)}{2\sqrt{\tau_c D_c}} > \sqrt{\alpha} \tag{3.9}$$

is a necessary condition.

We are not aware of a rigorous result concerning sufficient conditions for stability, even without production of surfactin (see, however, [7] for a formal stability analysis in this case).

The stability condition (3.9) shows that plateaus can be destabilized by a too strong production of surfactin, by a too large diffusivity of the chemoattractant, or if they are too short.

Shock profiles for small surfactin diffusivity

We examine the effect of a small surfactin diffusivity $0 < D_s \ll 1$ on the shape of traveling waves. Traveling wave solutions of (3.2) satisfy

$$\left.\begin{aligned} &-\sigma n' + \big((n(1-n)c' + nv\big)' = 0\,, \\ &-\sigma v' + \alpha n' = D_S v''\,, \\ &-D_c c'' + \tau_c c = n\,. \end{aligned}\right\} \tag{3.10}$$

Integration of the first two equations and the far field conditions $n(\pm\infty) = v(\pm\infty) = 0$ give

$$\left.\begin{aligned} &n\left(-\sigma + (1-n)c' + v\right) = 0\,, \\ &-\sigma v + \alpha n = D_S v'\,, \\ &-D_c c'' + \tau_c c = n\,. \end{aligned}\right\} \tag{3.11}$$

Now c, c', and v can be expected to be continuous, whereas n may still have jumps. The first two equations imply that these jumps have to be between regions, where

$$n = 0\,, \qquad D_S v' = -\sigma v\,, \tag{3.12}$$

and regions, where

$$n = 1 + \frac{v-\sigma}{c'}\,, \qquad D_S v' = \left(\frac{\alpha}{c'} - \sigma\right) v + \alpha\left(1 - \frac{\sigma}{c'}\right)\,. \tag{3.13}$$

Shock profile at the left jump: We shall construct shock profiles close to the jump points $y = 0$ and $y = L$ of the traveling wave of Theorem 3.1 and start with the left end of the wave at $y = 0$. By the smallness of D_S, the profile can be described asymptotically in terms of the boundary layer variable $\xi = y/D_S$. In the language of singular perturbation theory, v can be expected to be a fast variable, approximated as $v = v(\xi)$, whereas (for moderate values of D_c) c' is a slow variable, which can be approximated by the constant value $c'(0)$ (see (3.9)). The density n may have jumps between $n = 0$ and regions where, by (3.13), n is approximated by $n = 1+(v(\xi)-\sqrt{\alpha})/c'(0)$, since the wave speed is approximated by $\sigma = \sqrt{\alpha}$ as given in Theorem 3.1. We choose $\xi = 0$ as location of a jump from (3.12) to (3.13). For $\xi < 0$ we then have $dv/d\xi = -\sigma v$ subject to the matching condition $v(-\infty) = 0$, which has the unique solution $v(\xi) \equiv 0$. For $\xi > 0$, (3.13) implies

$$\frac{dv}{d\xi} = \mu_0(\sqrt{\alpha} - v)\,, \qquad \text{with} \quad \mu_0 = \sqrt{\alpha}\left(1 - \frac{\sqrt{\alpha}}{c'(0)}\right)\,,$$

subject to $v(0) = 0$ and to the matching condition $v(\infty) = \sqrt{\alpha}$. At this point we recover the stability condition $c'(0) > \sqrt{\alpha}$ of Theorem 3.2, which is necessary for solvability. If it is satisfied, we finally obtain the shock profile

$$n(\xi) = \begin{cases} 0 & \text{for } \xi < 0\,, \\ 1 - \frac{\sqrt{\alpha}}{c'(0)} e^{-\mu_0 \xi} & \text{for } \xi > 0\,, \end{cases} \quad v(\xi) = \begin{cases} 0 & \text{for } \xi < 0\,, \\ \sqrt{\alpha}\left(1 - e^{-\mu_0 \xi}\right) & \text{for } \xi > 0\,. \end{cases}$$

We reiterate that it contains a jump of n at $\xi = 0$.

Shock profile at the right jump: The construction of a shock profile at $y = L$ is similar. Now the boundary layer variable is given by $\eta = (y-L)/D_S$, and we search for a solution, where (3.13) holds for $\eta < 0$ and (3.12) for $\eta > 0$. Since $c'(L) < 0$, both differential equations for v have decaying solutions, again meaning that the only bounded solution for $\eta < 0$ is constant. This finally leads to the shock profile

$$n(\eta) = \begin{cases} 1 \text{ for } \eta < 0\,, \\ 0 \text{ for } \eta > 0\,, \end{cases} \quad v(\eta) = \begin{cases} \sqrt{\alpha} & \text{for } \eta < 0\,, \\ \sqrt{\alpha}\, e^{-\sqrt{\alpha}\,\eta} & \text{for } \eta > 0\,. \end{cases}$$

Note that now there is no profile in the swarmer density. An illustration of our qualitative results is given in Figure 2.

The theoretical predictions concerning the stability of the traveling waves have been examined by numerical simulations, which have been performed with $x \in [0, 7]$ and two sets of coefficients. Results are shown in Figure 3, where we can see (Figure 3a) the formation of the boundary layers as predicted above, when the stability condition is satisfied. Figure 3b shows the results of numerical simulations, when the stability condition is violated. We observe that the jump on the left side of the profile is replaced by a rarefaction wave.

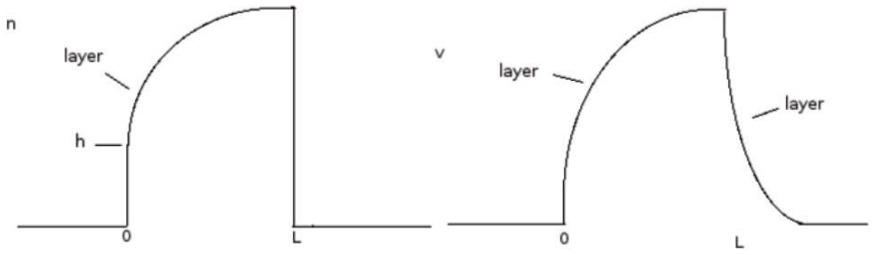

Figure 2. Qualitative representation of traveling plateau solutions of (3.2). Left: the swarmer density n, where $h = 1 - \frac{\sigma}{c'(0)}$ is the height of the jump on the left side of the front. Right: the gradient v of the surfactin concentration.

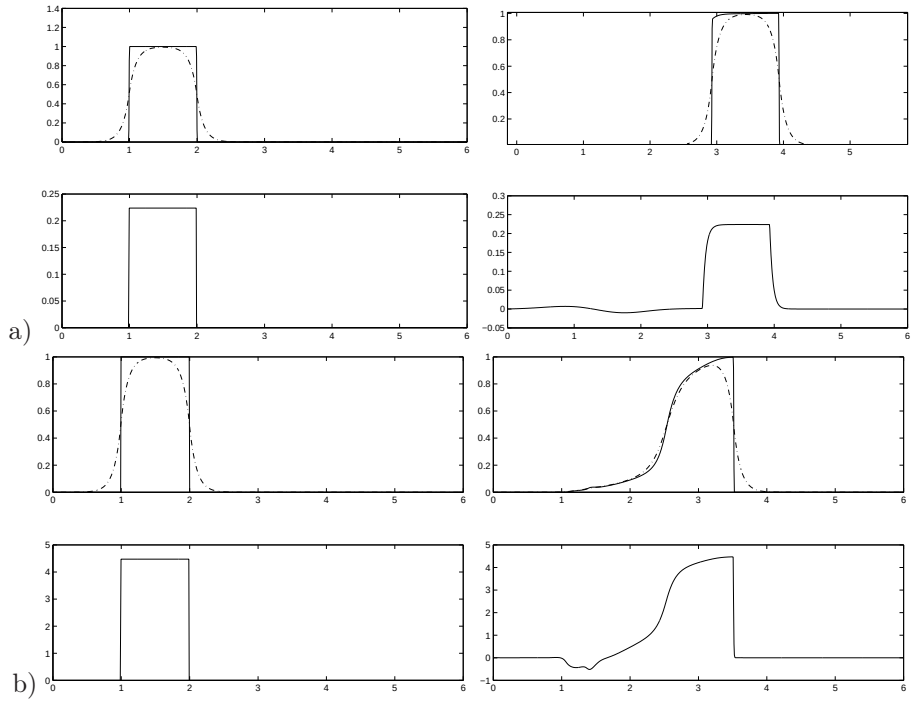

Figure 3. Numerical simulations of (3.2) with two sets of coefficients and the plateau wave of Theorem 3.1 as initial datum. The left column depicts the initial data for n and for the chemoattractant c by solid and dash dotted lines, respectively, (top) and for the gradient v of the surfactin concentration (bottom). The right column is a snapshot at a later time. a) $D_S = 0.01$, $\alpha = 0.05$, $\tau_c = 1$, and $D_c = 0.01$. In this case, the stability condition $c'(0) > \sqrt{\alpha}$ is satisfied. The results verify the qualitative picture in Figure 2. b) $D_S = 0.01$, $\alpha = 20$, $\tau_c = 1$, and $D_c = 0.01$. Now the stability condition is violated, the shock at the left is unstable and is replaced by a rarefaction wave.

4. Plateau splitting in reduced models

As we have seen, reduced models such as (3.1) can produce stable traveling plateaus for swarmers taht are compatible with the elongation of dendrites. In this section we show, based on numerical solutions, that reduced models are also able to produce instabilities and branching patterns. It turns out that the source term for S is crucial and we explore several possible forms. We will come back on mathematical questions of existence (in smallness regimes) in a forthcoming work [26].

4.1. *Reduced 1D model without supporters*

In the numerical results shown in Section 2, branching of dendrites is induced by the splitting of groups of swarmers transversal to the direction of movement. This section shows that splitting in the longitudinal direction is also possible. We consider an extension of the one-dimensional version of (3.1), where we incorporate the mother colony as an additional driving force and degradation of surfactin. This yields

$$\left.\begin{aligned} &\partial_t n + \partial_x\big(n(1-n)\partial_x c - n\partial_x S\big) = 0\,,\\ &-D_c\partial_x^2 c + \tau_c c = n\,,\\ &\partial_t S - D_S\partial_x^2 S + \tau_S S = \alpha_S m_{col} + \alpha n\,. \end{aligned}\right\} \tag{4.1}$$

Numerical simulations have been carried out with $0 \le x \le 9$ and with the mother colony $m_{col} = 3\chi_{[0,1]}$ (three times higher than the swarmer population density in accordance with the biophysical situation described in the introduction). The initial data for the swarmer density and for the surfactin concentration are given by $n_0 = \chi_{[1.5,2]}$ and, respectively, by the stationary solution of the surfactin equation with n replaced by n_0. Other model parameters are given in the figure caption. Results are depicted in Fig. 4. We observe a splitting of the swarmer colony occurring due to the combined effect of a drop of n in the plateau (due to the effect of the production of surfactin by the swarmers) and of the capability of the system to recreate plateaus that are separated by the external signal from the mother colony. In simulations with $\alpha = 0$, i.e. without production of surfactin by the swarmers (results not shown), splitting does not occur. The surfactin gradient just transports a plateau of swarmer cells.

4.2. *Reduced 2D model without supporters*

In this section we present numerical results for the two-dimensional version of (4.1) with $\alpha = 0$, i.e.,

$$\left.\begin{aligned} &\partial_t n + \mathrm{div}(n(1-n)\nabla c - n\nabla S) = 0\,,\\ &-D_c c + \tau_c c = \alpha_c n\,,\\ &\partial_t S - D_S\nabla^2 S + \tau_S S = \alpha_S m_{col}\,. \end{aligned}\right\} \tag{4.2}$$

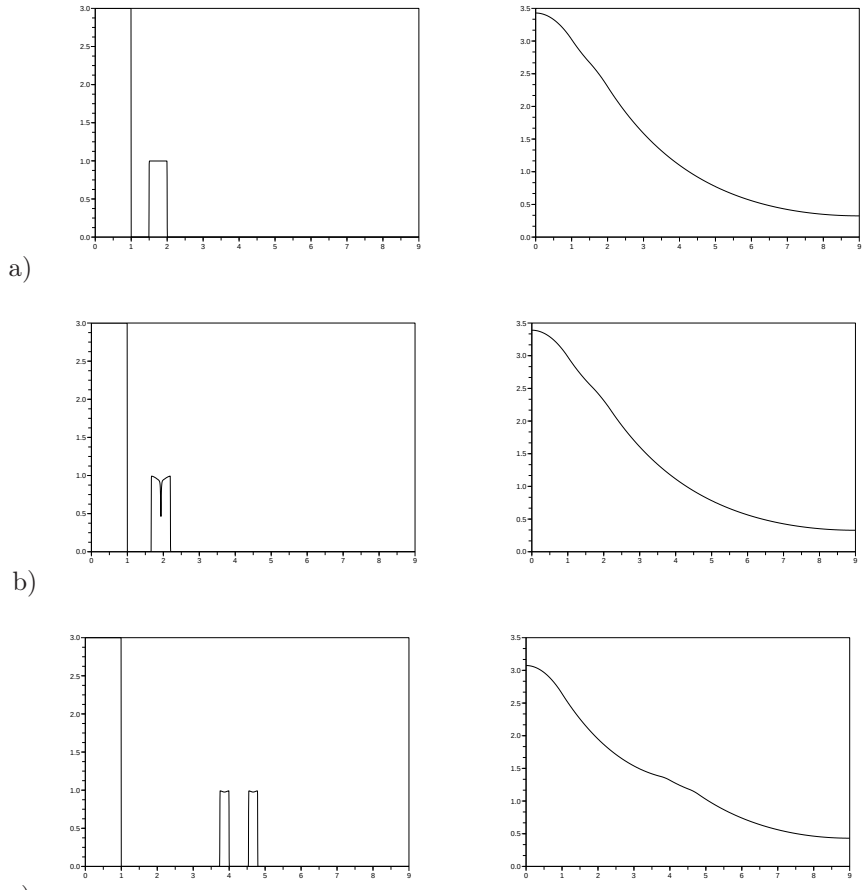

Figure 4. Numerical solution of (4.1) with $D_S = 7$, $\alpha_S = 6$, $\alpha = 3$, $\tau_S = \tau_c = 1$, $\alpha_c = 1$ and $D_c = 0.002$. The left column shows $n + m_{col}$ and the right column S: a) initial data, b) intermediate state, c) split state.

We emphasize the choice $\alpha = 0$, avoiding plateau splitting in the longitudinal direction, according to the results of the previous section. In two dimensions, however, transversal splitting may occur, which is the basis for dendrite branching. This is shown in Figure 5. The term $-\nabla S$ acts so as to stretch the initial plateau-like state transversally, as depicted in Fig. 5a). Once the stripe is too thin, the conservation of mass and the action of ∇c give rise to the splitting.

Here we have used $x \in [0,2]^2$, $\alpha = 0$, $D_S = 1$, $\tau_S = 10$, $\tau_c = 1$, $\alpha_c = 1$ and $D_c = 0.005$. The mother colony occupies the left bottom corner of the computational domain and we have chosen $m_{col} = 3\chi_{|x|\leq 0.2}$. The initial swarmer density is $n(0,x) = \chi_B$ with $B = \{x = (x_1, x_2) :\ (x_1 - 0.5)^2 + (x_2 - 0.5)^2 < 0.3^2,\ 0.4 < |x| < 0.6\}$, as displayed in Figure 5a).

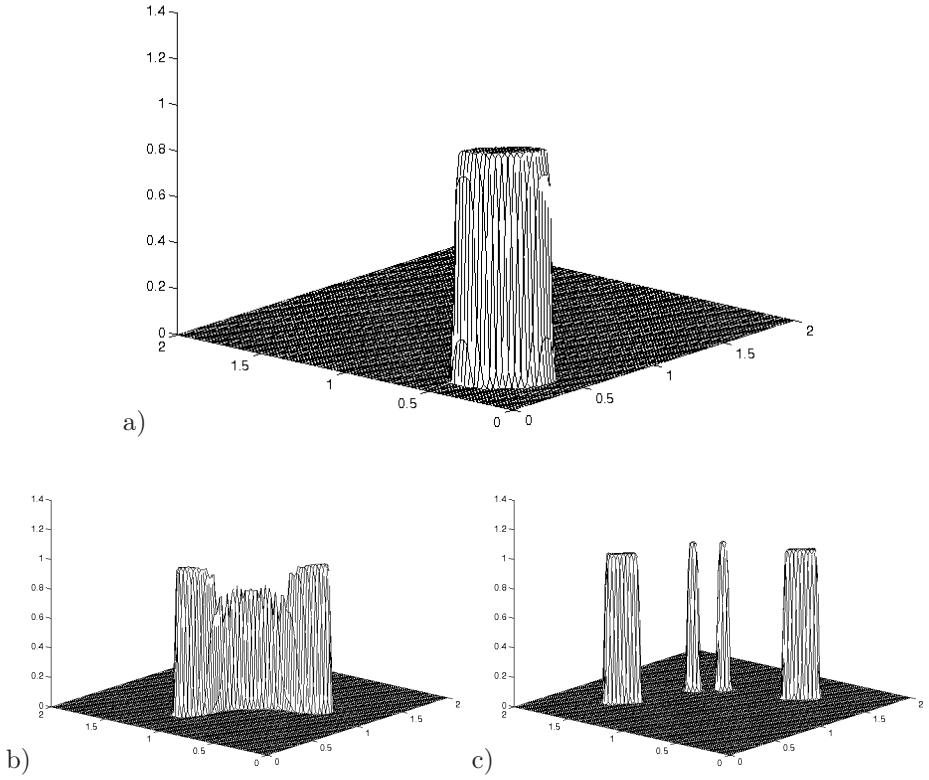

Figure 5. Numerical simulations of (4.2) with $x \in [0,2]^2$, $\alpha = 0$, $D_S = 1$, $\tau_S = 10$, $\tau_c = 1$, $\alpha_c = 1$, $D_c = 0.005$. The swarmer density is shown at different points in time: a) initial data, b) intermediate state, c) split state.

4.3. *Reduced 2D model with supporters*

The system considered now,

$$\left.\begin{aligned} &\partial_t n + \nabla(n(1-n)\nabla c - n\nabla S) = 0\,, \\ &-D_c c + \tau_c c = n\,, \\ &-D_S \Delta S + S = \alpha_S m_{col} + \alpha_f f\,, \\ &\partial_t f = B_f f(\beta - f) + B_n n\,, \end{aligned}\right\} \tag{4.3}$$

is almost the full system (2.1), however without the effect of supporter diffusion caused by a trace substance and with a quasistationary equation for the surfactin concentration. On the other hand, a logistic growth term for the supporters should have a similar effect of making the supporter concentration approximately constant.

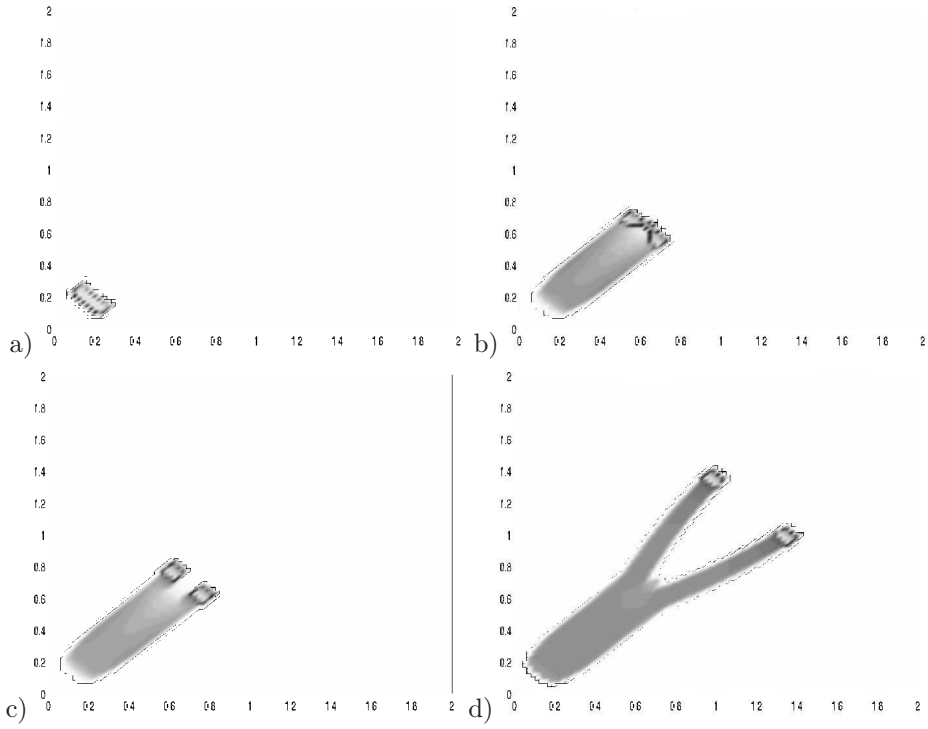

Figure 6. Time dynamic of swarmers plus supporters density computed with the 2d model (4.3) with supporter cells.

This is a mathematical simplification, which preserves this feature as can be seen in Fig. 6, but ignores the observed motility of supporter cells.

Moreover, taking the time derivative for the equation for S, one gets

$$\partial_t S = D_S \partial_t \Delta S + \alpha_f \partial_t f = D_S \partial_t \Delta S + \alpha_f B_f f(\beta - f) + \alpha_f B_n n\,,$$

so that when α_f is small and $D_S = 0$, (4.3) is a perturbation of the reduced traveling wave model (3.1). By the results of Section 3, this makes the existence of traveling wave solutions rather likely.

For a numerical solution, the parameters have been chosen as $L = 2$, $D_S = 0.05$, $D_c = 0.0005$, $\alpha_c = 2$, $\alpha_m = 1$, $\alpha_f = 2$, $B_f = 12$, $B_n = 4$, $\beta = 1/3$. The mother colony is still chosen as $m_{col} = 3\chi_{|x|<0.2}$. The initial conditions are $f(t=0) = 0$, $n(t=0) = \chi_B$ with $B = \{x = (x_1, x_2) :\ 0.2 < |x| < 0.3,\ (x_1 - 0.2)^2 + (x_2 - 0.2)^2 < 0.1^2\}$.

The results are shown in Fig. 6. This simplified model reproduces branching patterns similar to that of the full model (2.1), with a constant density of swarmers and supporters respectively in the tip and along the dendrite.

5. Conclusion

Dentritic patterns are commonly observed during the swarming of bacterial cells colonies such as *B. subtilis*. Established models to reproduce these patterns are usually based on parabolic equations, and the instability is driven by the local depletion of nutrient.

Here we have considered an hyperbolic model for the swarmer cells, which provides the leading mechanisms of the system, completed by various, possibly degenerate, parabolic equations for the other cells (in particular supporters) and for the chemicals excreted by these cells. But, motivated by experiments on rich media, no nutrient limitation is used.

New branching instabilities have been observed in the complete model including a mother colony, supporter cells and swarmers which has been devised based on former hyperbolic Keller-Segel with logistic sensitivity models proposed in [4,7]. Reduced models, more amenable to analysis, explain several numerical observations: traveling plateaus for the swarmers exist generically and are stable under size conditions in one space dimension. The instability mechanisms, responsible for branching, are numerous and depend on the dimension, where the computations are performed.

From the modeling side, improvement of the description of short range effects of surfactin is necessary, and we can expect different branching instabilities in more realistic systems. From the theoretical point of view, understanding two dimensional effects and further instability effects is certainly the most challenging problem.

Acknowledgements

This work was achieved as C. S. was visiting INRIA/UPMC team Bang on a visitor position. F. C. has been supported by the Marie Curie Actions of the European Commission in the frame of the DEASE project (MEST-CT-2005-021122).

Bibliography

1. `http://www.freefem.org/ff++`.
2. Bouchut F., *Nonlinear stability of finite volume methods for hyperbolic conservation laws and well-balanced schemes for sources*. Series Frontiers in Mathematics, Birkhäuser Verlag, Basel (2004).
3. M. Burger, M. Di Francesco, Y. Dolak-Struss, The Keller-Segel model with prevention of overcrowding: linear vs. nonlinear diffusion. SIAM J. Math. Anal. **38** No. 4, (2006) 1288-1315.
4. M. Burger, Y. Dolak-Struss, C. Schmeiser, Asymptotic analysis of an advection-dominated chemotaxis model in multiple spatial dimensions. Commun. Math. Sci. **6** No. 1,(2008) 1-28.
5. M. Burger, P. Markowich, J.-F. Pietschmann. Work in preparation.
6. A. L. Dalibard, B. Perthame, Existence of solutions of the hyperbolic Keller-Segel model. Trans. Amer. Math. Soc. **361** No. 5, (2009) 2319-2335.
7. Y. Dolak-Struss, C. Schmeiser, The Keller-Segel model with logistic sensitivity function and small diffusivity. SIAM J. Appl. Math., **66** No. 1, (2005) 286-308.

8. I. Golding, Y. Kozlovsky, I. Cohen, E. Ben-Jacob, Studies of bacterial branching growth using reaction-diffusion models for colonial development. Physica A **260**, (1998) 510-554.
9. P. Gray, S. K. Scott, Autocatalytic reactions in the isothermal continuous stirred tank reactor: isolas and other forms of multistability. Chem. Eng. Sci. **38**, no. 1, (1983) 29-43.
10. K. Hamze, D. Julkowska, S. Autret, K. Hinc et al., Identification of genes required for different stages of dentritic swarming in *Bacillus subtilis*, with a role for *phrC*. Microbiology **155**, (2009) 398-412.
11. T. Hillen, A classification of spikes and plateaus. SIAM Rev. **49**(1), (2007) 35-51.
12. T. Hillen, K. Painter, A user's guide to PDE models for chemotaxis. J. Math. Biol. **58**, (2009) 183-217.
13. D. Horstmann, From 1970 until present: The Keller-Segel model in chemotaxis and its consequences, Part I. Jahresbericht der DMV **105**, no. 3, (2003) 103-165.
14. D. Horstmann, From 1970 until present: The Keller-Segel model in chemotaxis and its consequences, Part II. Jahresbericht der DMV **106**, no. 2, (2004) 51-69.
15. D. Julkowska, M. Obuchowski, I. B. Holland, S. J. Seror, Branched swarming patterns on a synthetic medium formed by wild type Bacillus subtilis strain 3610. Microbiology **150**, (2004) 1839-1849 .
16. D. Julkowska, M. Obuchowski, I. B. Holland, S. J. Seror, Comparative analysis of the development of swarming communities Bacillus subtilis 168 anda a natural wild type: critical effect of the surfactin and the composition of the medium. J. Bacteriol. **187**, (2005) 65-74.
17. Y. Kozlovsky, I. Cohen, I. Golding, E. Ben-Jacob, Lubricating bacteria model for branching growth of bacterial colony. Phys. Rev. E, Phys. plasmas fluids Relat. Interdisciplinary Topics, **50**, (1999) 7025-7035.
18. D. A. Kessler, H. Levine, Fluctuation induced diffusive instabilities. Nature, **394**, (1998) 556-558.
19. K. Kawasaki, A. Mochizuki, M. Matsushita, T. Umeda, N. Shigesada, modeling spatio-temporal patterns created by Bacillus-subtilis. J. Theor. Biol., **188**, (1997) 177-185.
20. T. Li, Z. Wang, Nonlinear stability of traveling waves to a hyperbolic-parabolic system modeling chemotaxis. SIAM J. Appl. Math.**70**(5), 1522–1541 (2009).
21. A. Marrocco, H. Henry, I. B. Holland, M. Plapp, S. J. Séror, B. Perthame, Models of self-organizing bacterial communuities and comparisons with experimental observations. Math. Model. Nat. Phenom. Mathematical Modelling of Natural Phenomena Vol. 5 No 1 (2010), 148–162.
22. B. Maury, A. Roudneff-Chupin, F. Santambrogio, A macroscopic crowd motion model of gradient flow type. Math. Models Methods Appl. Sci., to appear.
23. M. Mimura, H. Sakaguchi, M. Matsushita, Reaction diffusion modeling of bacterial colony patterns. Physica A, **282**, (2000) 283-303.
24. J.D. Murray, Mathematical biology, Vol. 2, Second edition. Springer, 2002.
25. B. Perthame, *Transport equations in Biology* (LN Series Frontiers in Mathematics), Birkhauser, (2007).
26. B. Perthame, C. Schmeiser, M. Tang, N. Vauchelet. Traveling plateaus for a Keller-Segel system with logistic sensitivity; existence and branching instabilities. Work in preparation.
27. A. Sokolov, I. S. Aranson, J. O. Kessler, R. E. Goldstein, Concentration dependence of the collective dynamics of swimming bacteria. PRL **98**, 158102 (2007).
28. M. Winkler, Boundedness in the Higher-Dimensional Parabolic-Parabolic Chemotaxis

System with Logistic Source. Comm. Partial Diff. Eq. **35** (8) (2010) 1516–1537.